Development of an Image-guided Surgical Robot for Bone Tumor Resection*

Lingzhi Kong[1,2], Lei Cao[1], Yuanyuan Zhou[1], Yanjun Pei[3], Shuo Guo[3], Jun Fu[3], Lianqing Liu[1], Zheng Guo[3*] and Hao Liu[1*]

[1]State Key Laboratory of Robotics, Shenyang Institute of Automation, Chinese Academy of Sciences
[2]Northeastern University
Shenyang, China
[3] Department of Orthopaedics, Xijing Hospital, Fourth Military Medical University
Xi'an, China

***Abstract*—The conventional human-performed surgery of bone tumor resection has the drawbacks of imprecise, high labor intense on surgeons, longer recovery time. In this paper, a surgical robot system for bone tumor resection is developed. First the preoperative image of experimental bone is obtained by CT scanning. Then the surgeon is able to plan a surgery path by means of choosing key points on the 3D bone model. Second the relationship between image space and surgical space is established. Finally the surgery path made by the surgeon in image space is mapped to surgical space and robot can receive the commands to operate the surgery. Meanwhile, the position of the surgical tool is displayed in image space in real time. Acetabular bone and thigh bone trials were performed at hospital and the outcome shows the feasibility of using robot to resect bone tumor.**

Keywords—Surgical Robot; Image-guided surgery; Bone Tumor Resection; Precision Surgery

I. INTRODUCTION

The conventional treatment of bone tumor in clinical settings is using bone drill, osteotome and fretsaw to remove the lesion bone [1]. However, the drawbacks of traditional clinical treatment on bone tumor are imprecise, highly labor intense on medics, more damaging on patients, relying on surgeon's experience and "surgical feel". These problems inspire us to search for an alternative method to remove bone tumor.

With advantages such as higher precision, minimally invasive, robotic surgery delivers the goods in ways that traditional human-performed surgery (or, at least, some specific surgeries) cannot manage. Since the use of robotics in surgery in the mid-1980s, several orthopedic robots have been developed.

Robotic surgery has performed well in orthopedic surgery. Significant advances have been made in orthopaedic robots, both academically and technologically. Robotic surgery has been widely adopted as the treatment of several orthopedic diseases such as total knee arthroplasty, total hip replacement surgery, dental operation, spine surgery, etc [2] [8][10]. IBM developed an image-guided surgical robot for total hip replacement, which is the first active robot in any surgical field that performs a certain part of the procedure [3]. Mazor surgical technologies developed an image-guided robotics system for spine surgery which is already in clinical use for accurate guidance of spinal implant placements, such as pedicle screws and translaminar facet screws [9].

However, studies focusing on robotic surgery on bone tumor are limited [5][6]. Reijnders et al. provided the surgical oncologist with a new means of performing safe and radical sarcoma surgery with the help of image guidance technology [5]. Wong et al. worked on preoperative image analysis and planning of navigation computer-assisted bone tumor resection and reconstruction[7]. As far as we know, there is no researcher or company concerned about utilizing robotic surgery technology on bone tumor resection.

Performing the bone tumor resection procedure by means of robots offers a two-fold bonus: higher resection precision and less labor intense on surgeons. Moreover, a crucial procedure after performing the bone tumor resection surgery is bone allograft, namely, selecting a suitable bone from the bone bank and cutting it into the shape befitted the bone defect of the patient [1]. The effect of bone allograft is crucial to mechanical property which influences the stability of the bone. The human-performed bone allograft procedure cannot accurately ensure the shape as well as the angle of the margin which are of great importance, whereas robotic-aided surgery is capable to control the cutting position and angle with high precision.

Thus, we developed a low-cost surgical robot for bone tumor resection and performed several in vitro trials at hospital to evaluate the feasibility of using a robot to resect the bone tumor. First we load the 3D preoperative reconstructed image of the experimental bone. Then the surgeon could make a surgical path by means of choosing key points. Second we build the relationship between image space and surgical space. Finally we map the surgery path planned by the surgeon from image space to surgical space and command the robot to operate the surgery, meanwhile, the position of the surgery tool is displayed in image space.

The layout of the paper is as follows. Section II details the principle of the procedure of our system. Section III shows the details and outcome of the experiments performed at hospital. Section IV is the discussion and conclusion of our experiments and future work we intend to do.

This work was supported by National Natural Science Foundation of China (No. 61473281 and No. 61503370), Shenyang Double-hundred Engineering Project (No. Y7L1170101), corresponding to Zheng Guo (guozheng@fmmu.edu.cn), Hao Liu (liuhao@sia.cn).

II. Materials & Methods

Fig. 1 presents an overview of the Image-guided surgical robot system, which consists of the image guidance module and the Universal Robot 5 (UR5). The image guidance module is developed based on 3D Slicer which is a free and open source software package for image analysis and scientific visualization [12]. Then a handheld electric drill is mounted as an end effector of UR5 to perform the bone tumor resection surgery. The following sections provide the details of the system.

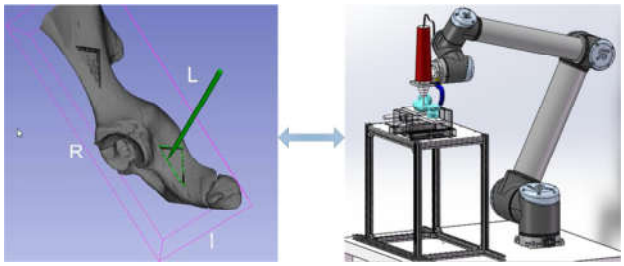

Fig. 1. The architecture of the system which consists of planning and visualization software, UR5 with surgical tool, cooling pipe, experimental bone, and fixture for fixing the bone.

A. Peoperative Planning

The DICOM image of the experimental bone is obtained by CT scanning. Then it is reconstructed in 3-dimentional STL format. The STL model of the experimental bone is imported to 3D Slicer so that the surgeon is able to select the key points to arrange a surgical path. The key points can be selected simply by click on the surface of the 3D model. After key point selection is done, a continuous closed spline curve is generated by these key points through spline curve fitting algorithm.

An issue here is that the surgical tool tip has a certain radius, say R, so we have to offset the surgical path along the vector V_{offset} that is perpendicular to the plane formed by tangential vector of the surgical path V_{Path} and the orientation vector of the surgical tool V_{Tool}. The orientation of the vector V_{offset} can be either towards the centroid of the surgical path or on the contrary, and the desired one is towards the centroid of the surgical path. Since the direction of V_{Path} is determined by the sequence of the key points which remains uncertainty, to obtain the desired orientation of V_{offset}, the centroid of the path P_C is calculated, and then we calculate the angle of V_{Path} and the vector V_{CP} formed by P_C and the point on the path P_P. If the angle $\theta > \pi/2$, the vector V_{offset} can be calculated by (1).

$$V_{offset} = -V_{Tool} \times V_{Path} \tag{1}$$

If the angle $\theta < \pi/2$, the vector V_{offset} can be calculated by (2).

$$V_{offset} = V_{Tool} \times V_{Path} \tag{2}$$

B. Surgical Tool Calibration

First, the relationship between the tool coordinate and the base coordinate of the robot must be calculated, which is a crucial step for the precision of the operation. Four-point calibration method is used in this system.

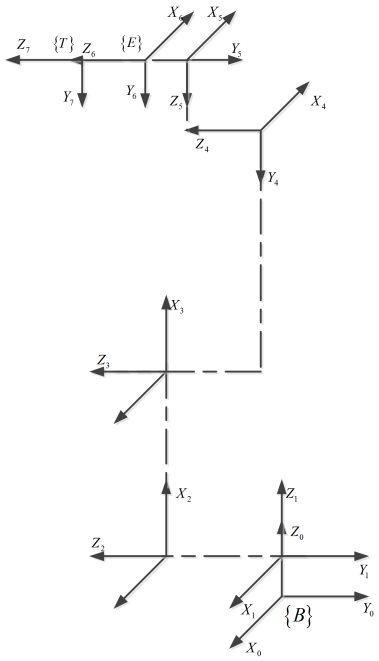

Fig. 2. Coordinate system of robot platform

The coordinate system of robot side is established as shown in Fig. 2, where {B} represents the base coordinate system of the robot, {E} represents the end flange coordinate system of the robot and {T} represents the tool coordinate system.

The relationship between {B} and {E} can be derived from (1), where ${}^{B}_{T}T$ represents the transformation matrix from {B} to {T}, ${}^{B}_{E}T$ represents the transformation matrix from {B} to {E}, ${}^{E}_{T}T$ represents the transformation matrix from {E} to {T}. Assume that the orientation transformation matrices of ${}^{B}_{T}T, {}^{B}_{E}T, {}^{E}_{T}T$ are ${}^{B}_{T}R$, ${}^{B}_{E}R$, ${}^{E}_{T}R$ respectively, and the translational vectors of ${}^{B}_{T}T, {}^{B}_{E}T, {}^{E}_{T}T$ are ${}^{B}_{T}P$, ${}^{B}_{E}P$, ${}^{E}_{T}P$ respectively. Then (3) can be expressed as (4), so we can get (5) . We assume that ${}^{B}_{T}\mathrm{R}$ is identity matrix.

$${}^{B}_{T}T = {}^{B}_{E}T\,{}^{E}_{T}T \tag{3}$$

$$\begin{bmatrix} {}^{B}_{T}R & {}^{B}_{T}P \\ 0 & 1 \end{bmatrix} = \begin{bmatrix} {}^{B}_{E}R & {}^{B}_{E}P \\ 0 & 1 \end{bmatrix} \cdot \begin{bmatrix} {}^{E}_{T}R & {}^{E}_{T}P \\ 0 & 1 \end{bmatrix} \tag{4}$$

$${}^{B}_{E}R \cdot {}^{E}_{T}P + {}^{B}_{E}P = {}^{B}_{T}P \tag{5}$$

Four different ${}^{B}_{E}R$ s can be achieved through the end effector of the tool to touch a fixed point from four different

orientations and (6) can be got due to the equality of the four ${}^{B}_{T}P$ s.

$$\begin{bmatrix} {}^{B}_{E}R_2 - {}^{B}_{E}R_1 \\ {}^{B}_{E}R_3 - {}^{B}_{E}R_2 \\ {}^{B}_{E}R_4 - {}^{B}_{E}R_3 \end{bmatrix} {}^{E}_{T}P = \begin{bmatrix} {}^{B}_{E}P_1 - {}^{B}_{E}P_2 \\ {}^{B}_{E}P_2 - {}^{B}_{E}P_3 \\ {}^{B}_{E}P_3 - {}^{B}_{E}P_4 \end{bmatrix} \tag{6}$$

Let

$$\mathrm{A} = \begin{bmatrix} {}^{B}_{E}R_2 - {}^{B}_{E}R_1 \\ {}^{B}_{E}R_3 - {}^{B}_{E}R_2 \\ {}^{B}_{E}R_4 - {}^{B}_{E}R_3 \end{bmatrix}, \quad B = \begin{bmatrix} {}^{B}_{E}P_1 - {}^{B}_{E}P_2 \\ {}^{B}_{E}P_2 - {}^{B}_{E}P_3 \\ {}^{B}_{E}P_3 - {}^{B}_{E}P_4 \end{bmatrix} \tag{7}$$

So ${}^{E}_{T}P$ can be got by means of least square method. The surgical tool calibration is done.

$${}^{E}_{T}P = (A^T A)^{-1} A^T B \tag{8}$$

Thus, the transformation matrix from the end flange of UR5 coordinate to surgical tool coordinate can be expressed as:

$${}^{T}T_{E} = \begin{bmatrix} & {}^{E}_{T}R & & {}^{E}_{T}P \\ 0 & 0 & 0 & 1 \end{bmatrix} \tag{9}$$

C. Registration

The registration algorithm consists of two steps: preregistration and accurate registration. Before CT scanning, four points are marked on the experimental bone so that the mark points can be seen in the reconstructed 3D model of the bone. These four points is used for preregistration.

Two groups of point clouds in robot space and image space are required to calculate the relationship between robot space and image space. The point cloud in robot space is obtained by means of touching the surface of the experimental bone through the surgical tool. And the point cloud in image space is obtained in 3D Slicer software. These two groups of point clouds can't be one-to-one correspondence due to the error in robot space.

Preregistration:

The four marked points in robot space and image space form two matrices P_r^M and P_i^M, respectively, as shown in (10) and (11).

$$P_r^M = \begin{bmatrix} x_r^1 & x_r^2 & x_r^3 & x_r^4 \\ y_r^1 & y_r^2 & y_r^3 & y_r^4 \\ z_r^1 & z_r^2 & z_r^3 & z_r^4 \\ 1 & 1 & 1 & 1 \end{bmatrix} \tag{10}$$

$$P_i^M = \begin{bmatrix} x_i^1 & x_i^2 & x_i^3 & x_i^4 \\ y_i^1 & y_i^2 & y_i^3 & y_i^4 \\ z_i^1 & z_i^2 & z_i^3 & z_i^4 \\ 1 & 1 & 1 & 1 \end{bmatrix} \tag{11}$$

Obviously, (12) is always true, so the preregistration matrix ${}^{i}T_{r}^{1}$ is shown in (13).

$$P_i^M = P_i^M (P_r^M)^{-1} P_r^M \tag{12}$$

$${}^{i}T_{r}^{\mathrm{pre}} = P_i^M (P_r^M)^{-1} \tag{13}$$

After the preregistration matrix is obtained, the point cloud in robot space P_r can be converted to P_r^{pre}, as shown in (14). Then the preregistration is completed.

$$P_r^{\mathrm{pre}} = {}^{i}T_r^{\mathrm{pre}} P_r \tag{14}$$

Accurate registration:

After preregistration, ICP registration algorithm is used to accomplish accurate registration, which was first proposed by Besl and Mckay, the essence of which is based on least squares registration, the rotation matrix R and the position vector P are updated until (15) is satisfied [3].

$$f(R,T) = \sum_{i=1}^{n} \left\| P_i^k - (RP_r^k + T) \right\|^2 = \min \tag{15}$$

The inputs of ICP algorithm are P_r^{pre} and image point cloud P_i. Basing on ICP registration algorithm, we can get the registration matrix (16). Then the point cloud P_r^{pre} can be matched to image point cloud P_i as shown in (17).

$${}^{r}T_{i}^{\mathrm{ac}} = \begin{bmatrix} & R & & T \\ 0 & 0 & 0 & 1 \end{bmatrix} \tag{16}$$

$$P_r^{pre} = {}^{r}T_i^{\mathrm{ac}} P_i \tag{17}$$

After precise registration is done, the registration matrix can be calculated through (18). Then the relationship between image space and surgical space is established.

$${}^{r}T_i = ({}^{i}T_r^{\mathrm{pre}})^{-1} {}^{i}T_r^{ac} \tag{18}$$

D. Bone Tumor Resection and Surgery Visualization

In section C, the transformation matrix from image coordinate to robot coordinate can be got, which leads to the feasibility of mapping the preoperative planning path to robot space. We display the surgery tool in image space by vtk cone. The position of surgical tool in image space is calculated by means of multiplying inverse transformation matrix by tool orientation and position.

III. EXPERIMENTS

Our experiment platform consists of a UR5 (Universal Robot 5), an electric drill, a cooling pipe for cooling the drill tool, an acetabular bone, and a robot controller, , as shown in Fig. 3. The robot was controlled through a 64-bit windows 7 PC with an AMD 10 processor with 4GB RAM. We developed a server to send commands to UR5 to control the robot and receive data from UR5 for visualization of the surgery via TCP/IP network protocol and transferred the data received from UR5 to image space. The robot control server was integrated to 3D Slicer. The experiments were performed at hospital.

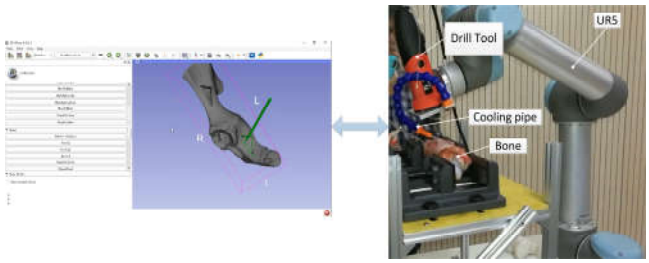

Fig. 3. The experiment platform

The preoperative CT data of the experimental bone was reconstructed in 3-dimentional STL format which was imported to 3D Slicer. The image guidance model was implemented in python as a scripted module for 3D Slicer, as shown in Fig. 4, which consists of a control panel (on left side) for surgeons to control the operation procedure and 3D visual guidance view for surgeons to plan surgical path and provide visualization of the surgery.

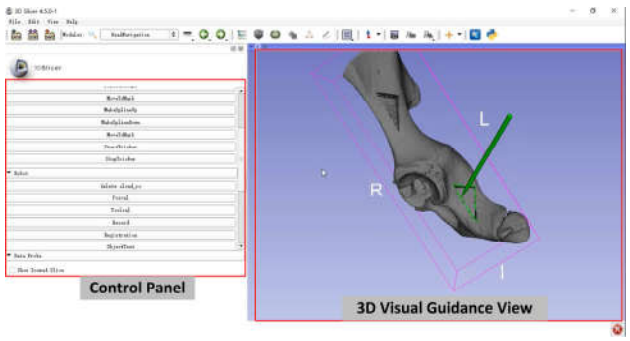

Fig. 4. Robot control and image guidance software is integrated in 3D Slicer, which consists of control panel (on left side) and 3D visual guidance view (on right side)

A. Surgical Path Generation

The reconstructed STL model of the experimental bone was imported to 3D Slicer. Then the surgeon could select key points on the surface of the bone STL model to make surgical path. Fig. 5 presents the selected key points(upper) and the surgical path generated by these points(below). We used the spline function of the visualization toolkit to generate a spine curve [11].

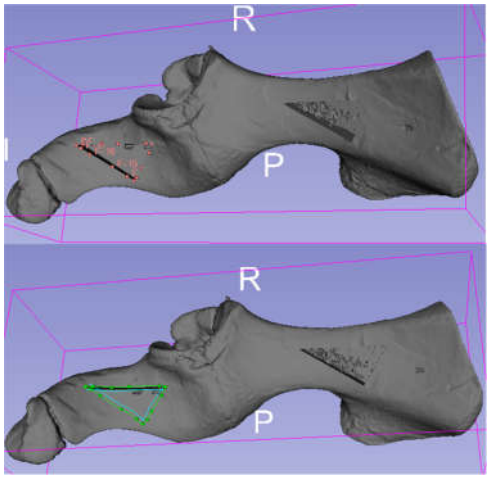

Fig. 5. Surgical path planning

B. Point Clouds Acquiring

We first selected the four marked points in sequence on the surface of the STL bone model and the experimental bone respectively and recorded their coordinate value. Then we selected a group of point cloud randomly on the surface of the STL bone model in image space and a group of point cloud on the surface of experimental bone in surgical space, as shown in Fig. 6.

After the surgical path has been generated, another key problem is to convert the path curve from image space to surgical space. The image space and surgical space corresponded to each other through two-step registration method: preregistration and precise registration.

The first four selected mark points were used for preregistration, and the whole point cloud was used for precise registration. After the whole calculation had been finished, we could convert the path curve in image space to surgical space and also could convert the surgical tool position in surgical space to image space for surgical tool position visualization.

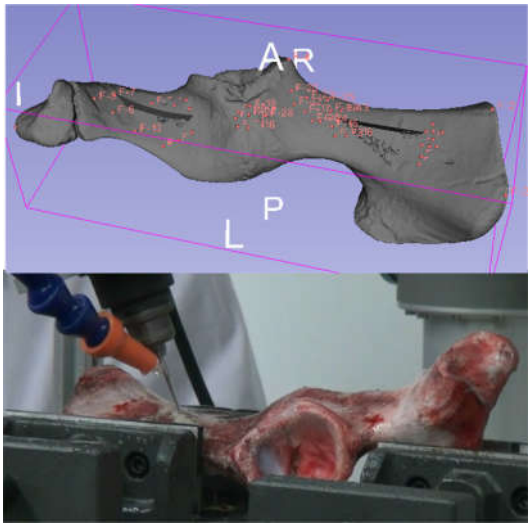

Fig. 6. Point clouds acquiring, upper of which is point cloud in image space, below of which is point cloud selection in surgical space

C. Surgery Procedure

Since the path curve is a continuous closed curve, we used the interpolation method to approximate the path curve with a certain number of points, say twenty. So we converted the group of points from image space to surgical space and then commanded UR5 to get to the converted points to complete the surgical procedure. During the procedure, the surgical tool position could be displayed in 3D image guidance view in real time. We have performed the experiments with acetabular bone and thigh bone, as shown in Fig. 7 and Fig. 8. The cutting procedure would be made step by step, precisely speaking, 1mm, because of the insufficient stiffness of the drill bit.

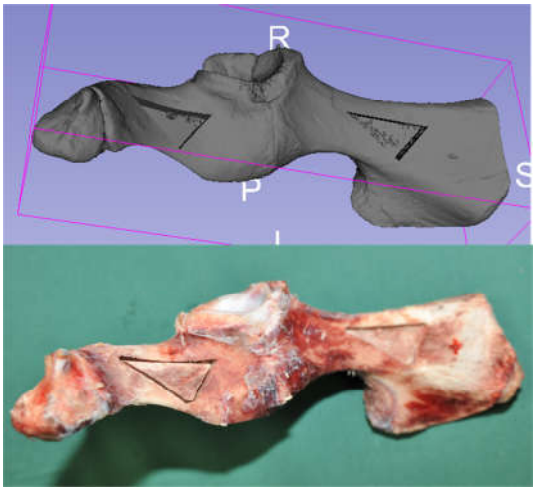

Fig. 7. Experimental outcome on acetabular bone, upper is the path in image space and below is the path in surgical space

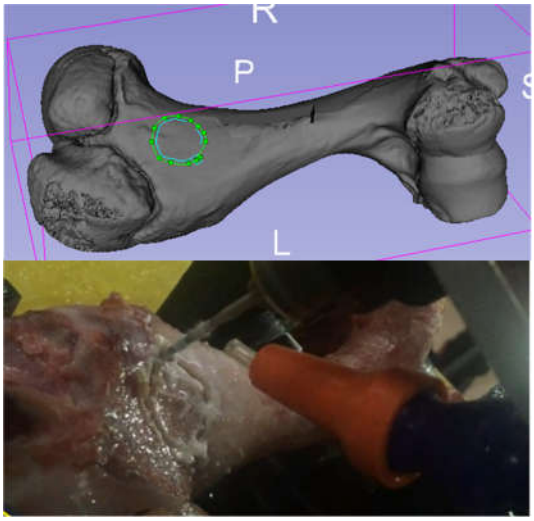

Fig. 8. Experiment outcome on thigh bone, upper is the path in image space and below is the path in surgical space

D. Outcome

To measure the gaps between the 3D model and the bone, we selected 5 key points on the path curve and compared their differences between the planned path curve in image space and the actual resection path curve, as shown in TABLE I.

TABLE I. DIFFERENCES BETWEEN THE PLANNED AND ACTUAL RESECTION PATH CURVE

	Point position disparities				
	k_1	k_2	k_3	k_4	k_5
Error(mm)	1.4	1.2	1.4	0.9	1.7

The mean error between the planned and actual resection path curve is 1.32mm. The outcome shows that using a robot to operate bone tumor resection surgery can observably increase the accuracy of the surgery compared with conventional human-performed surgery.

IV. CONCLUSION & DISCUSSION

In this study, we developed a surgical robot for bone tumor resection and performed several in vitro experiments at hospital. The outcome shows the feasibility of operating bone tumor resection surgery through image-guided robot. There are several issues raised in the experiments. The first one is that the drill bit may be sheared off during the procedure. To solve this problem, we intend to mount a six-axis force sensor onto the end flange of UR5 and utilize the data of force sensor to control the robot for the purpose of improving the safety of the system and preventing the potential damage of surgical tool. The error of the procedure comes from several aspects such as CT scanning accuracy, surgical tool calibration accuracy, registration accuracy.

Still, some improvements on software need to be made to make it easier for surgeons to operate. Integrated graphical user interface for surgeon use need to be developed and the software should be rewritten in industrial-standard language. Future works include improving the safety of the system and considering disinfection matters to make it applied in clinical settings.

ACKNOWLEDGMENT

Siwen Hao and Xu Zhang assisted with the mechanical design of the adapter and cooling system of the surgical tool.

REFERENCES

[1] Wei Guo, "Bone Tumor Surgery, "People's Medical Publishing House, 3:1032-1052, 2015.

[2] H. A. Paul, W. L. Bargar, B. Mittlestadt, B. Musits, R. H. Taylor, P. Kazanzides, et al., "Development of a Surgical Robot for Cementless Total Hip Arthroplasty," Clinical Orthopaedics and Related Research, vol. 285, pp. 57-66, 1992.

[3] W. L. Bargar, A. Bauer, and M. Börner, "Primary and Revision Total Hip Replacement Using the Robodoc (R) System," Clinical orthopaedics and related research, vol. 354, pp. 82-91, 1998.

[4] P. J. Besl and N. D. McKay, "A method for registration of 3-D shapes," IEEE Transactions on pattern analysis and machine intelligence, vol. 14, pp. 239-256, 1992.

[5] K. Reijnders, M. H. Coppes, A. L. J. van Hulzen, J. P. Gravendeel, R. J. van Ginkel, and H. J. Hoekstra, "Image guided surgery: New technology for surgery of soft tissue and bone sarcomas," European Journal of Surgical Oncology (EJSO), vol. 33, pp. 390-398, 2007/04/01/ 2007.

[6] Xiaohui Niu, "How to Understand the Role of Computer Navigation System in Bone Tumor Surgery," Chinese Journal of Clinicians, 2012,06(12):3170-3171.DOI:10.3877/cma.j.issn.1674-0785.2012.12.003.

[7] K. C. Wong, S. M. Kumta, G. E. Antonio, and L. F. Tse, "Image Fusion for Computer-assisted Bone Tumor Surgery," Clinical Orthopaedics and Related Research, vol. 466, pp. 2533-2541, 07/22

[8] P. Merloz, J. Tonetti, L. Pittet, M. Coulomb, S. Lavalleé, and P. Sautot, "Pedicle Screw Placement Using Image Guided Techniques," Clinical Orthopaedics and Related Research, vol. 354, pp. 39-48, 1998.

[9] M. Shoham, S. Brink-Danan, A. Friedlander, and N. Knoller, "Bone-Mounted Miniature Robotic System for Spine Surgery," in The First IEEE/RAS-EMBS International Conference on Biomedical Robotics and Biomechatronics, 2006. BioRob 2006., 2006, pp. 917-920.

[10] M. Sießegger, B. T. Schneider, R. A. Mischkowski, F. Lazar, B. Krug, B. Klesper, et al., "Use of an image-guided navigation system in dental implant surgery in anatomically complex operation sites," Journal of Cranio-Maxillofacial Surgery, vol. 29, pp. 276-281, 2001.

[11] http://www.vtk.org/vtk-users-guide/

[12] https://www.slicer.org/wiki/Documentation/4.5